frontiers | Frontiers in Energy Research

TYPE Original Research
PUBLISHED 12 February 2024
DOI 10.3389/fenrg.2024.1326466

OPEN ACCESS

EDITED BY
Marcin Debowski,
University of Warmia and Mazury in Olsztyn, Poland

REVIEWED BY
Geetesh Goga,
Bharat Group of Colleges, India
Praveenkumar T. R,
Graphic Era University, India

*CORRESPONDENCE
Bengi Şanlı,
bengigozmen@mersin.edu.tr

RECEIVED 23 October 2023
ACCEPTED 23 January 2024
PUBLISHED 12 February 2024

CITATION
Şanlı B, Güven O, Özcanlı M and Uludamar E (2024), Determining the effect of tung biodiesel on thermodynamic, thermoeconomic, and exergoeconomic analyses at high engine speeds.
Front. Energy Res. 12:1326466.
doi: 10.3389/fenrg.2024.1326466

Determining the effect of tung biodiesel on thermodynamic, thermoeconomic, and exergoeconomic analyses at high engine speeds

Bengi Şanlı[1]*, Onur Güven[1], Mustafa Özcanlı[2] and Erinç Uludamar[3]

[1]Mersin University, Department of Mechanical Engineering, Mersin, Türkiye, [2]Cukurova University, Department of Automotive Engineering, Adana, Türkiye, [3]Adana Alparslan Türkeş Science and Technology University, Department of Mechanical Engineering, Adana, Türkiye

Tung biodiesel is a promising alternative fuel type produced from the tung tree. In the current study, the effect of the addition of 20%, by volume, of tung biodiesel to diesel fuel was evaluated in terms of energetic–exergetic analyses based on the first and second laws of thermodynamic at various high engine speeds (2,400, 2,600, and 2,800 rpm). Additionally, this study aimed to assess the thermoeconomic and exergoeconomic aspects of a diesel engine. The findings revealed that the amount of energy converted to useful work for the diesel fuel was higher than that of the DTB20 fuel, even though the fuel energy obtained from DTB20 fuel was higher than that of diesel fuel at all engine speeds. The highest energy and exergy efficiencies for the engine fueled with diesel fuel were obtained as 31.07% and 29.15% respectively, while the corresponding values for the engine fueled with DTB20 fuel were determined as 27.15% and 25.19% at the engine speed of 2,400 rpm, respectively. However, at 2,800 rpm, a significant decrease in both the energy and exergy efficiencies was observed for both diesel and tung biodiesel blended fuels due to the increased mechanical friction of the engine components. Furthermore, at the highest engine speed, entropy generation increased, owing to a higher exergy destruction rate. The entropy generation rate increased to 0.38 kW/K for diesel fuel and 0.46 kW/K for DTB20 fuel since the enhancement of the engine speed caused the ascent of the fuel consumption rate. Regarding thermoeconomic–exergoeconomic analyses, for both diesel and tung biodiesel blended fuels, there is no distinct difference in the thermoeconomic–exergoeconomic parameters at 2,400 and 2,600 rpm as the values of these parameters at the engine speed of 2,800 rpm increased significantly. In light of all the findings, it can be concluded that the engine speed of 2,800 rpm is not applicable to run the engine due to higher friction and corresponding energy destruction in the engine system.

KEYWORDS

energetic, exergetic, thermoeconomic, exergoeconomic, tung, biodiesel

1 Introduction

Energy demand and consumption have been continuously increasing year by year due to the social–economic progress of countries (Li et al., 2023). Diesel engines dominate the power generation and transportation sectors to meet this demand (El-adawy, 2023; Goyal et al., 2023). However, their consumption has led to the release of harmful emissions from the diesel engine to the environment (Goga et al., 2021). Investigations have been carried out to pinpoint environmentally friendly, renewable, and sustainable energy sources. Biofuels are the mainstay of these studies (Jain et al., 2023a). For diesel engines, biodiesel, which can be obtained from various plant sources, animal fats, and waste oils, is an important alternative fuel to fossil-based diesel fuels as it is non-toxic and reduces carbon monoxide and hydrocarbon emissions (Aslan, 2023; Kumar and Gautam, 2023; Liu et al., 2023; Raj Bukkarapu and Krishnasamy, 2023; Xu et al., 2023). The similar physical properties of lower blends of biodiesels bring about an attractive alternative fuel to conventional diesel fuels. According to the previous studies, the physicochemical properties of various biodiesel fuels are given in Table 1.

The studies mostly examined the performance and emission characteristics of biodiesel-fueled engines. In these studies, it was found that several advantages are associated with biodiesel use, including reduced levels of unburnt hydrocarbons (HCs) and carbon monoxide (CO), and smoke opacity. However, nitrogen oxides (NOx) and brake-specific fuel consumption (BSFC), along with certain performance parameters, were generally adversely affected (Kukana and Jakhar, 2022; Kumar et al., 2023).

The studies about tung biodiesel-fueled diesel fuel were performed by researchers. In those studies, Harish et al. (2019) found out that the properties of tung biodiesel are close to a conventional diesel. The biodiesel exposed lower NO_x and HC emissions, while the brake thermal efficiency (BTE) and BSFC do not show significant variations when compared with the diesel fuel (Harish et al., 2019). In the studies of Celebi et al. (2017), they compared it to conventional diesel fuels; BSFC increased up to 12.37% with tung biodiesel and up to 18.31% at low- and medium-load conditions, respectively, and a reduction of up to 6.15% in the engine vibration was observed by the researchers (Celebi et al., 2017).

Although most of the studies on biodiesel-fueled diesel engines have focused on engine performance and emission characteristics, this is insufficient for a comprehensive understanding of the engine behavior. To gain insights into all aspects of the energy flow within the engine, the second law of thermodynamics should be considered. Consequently, the literature includes various exergy and energy analyses of diesel engines fueled with biodiesel from various sources. Energy–exergy emission analysis of a *Spirulina* microalgae biodiesel-fueled diesel engine was performed by Rajpoot et al. (2023). They used pure diesel, 20% and 80% blends, and pure biodiesel fuels when the engine was loaded as 25%, 50%, 75%, and 100% at 1,500 rpm. They found out that the highest energy and exergy efficiencies were 33.55% and 31.48%, respectively. With *Spirulina* microalgae biodiesel usage, the highest energy efficiencies were 33.02% for a 20% blend, 32.80% for an 80% blend, and 31.89% for pure biodiesel, while the highest exergy efficiencies were 30.77% for the 20% blend, 30.43% for the 80% blend, and 29.51% for pure biodiesel at full load. *Jatropha* biodiesel was used by Rawat et al. (2023). In this study, they fueled the diesel engine with an ethanol–jatropha biodiesel blend and added hydrogen fuel. During the experiments, they loaded the engine as 25%, 50%, 75%, and 100% at 1,500 rpm with five different hydrogen injection durations. According to their results, hydrogen addition to 10% ethanol + 90% jatropha biodiesel had a higher energetic efficiency than pure diesel fuel. Odibi et al. (2019) used waste cooking biodiesel and triacetin as oxygenated fuels in their turbo-charged, six-cylinder diesel engine. According to their results, biodiesel had a higher thermal and the lowest exhaust loss fraction. Furthermore, oxygenate fuels resulted in a higher exergetic efficiency of up to 10% (Odibi et al., 2019). Nabi et al. (2019) used biodiesels from waste cooking oil and macadamia oil. In the experiments, they fueled a four-stroke, four-cylinder, naturally aspirated diesel engine (Nabi et al., 2019). The results indicated that fuel energy and exergy were slightly decreased with biodiesel usage due to their lower heating values. In the study of Cavalcanti et al. (2019), they performed exergy, exergoeconomic, and exergoenvironmental analyses (Cavalcanti et al., 2019). They found that 5% and 25% biodiesel concentrations, in volume, had the highest exergy performances as 33.09% and 33.33%, respectively. The exergoeconomic factor, which is the lowest value with pure biodiesel usage, decreased with the increment of exergy losses and destruction. Furthermore, a higher biodiesel ratio led to lower environmental impacts and higher exergoenvironmental factors.

The tung tree (*Vernicia fordii*) is native to southern China (Suzuki et al., 2021). The oil extracted from the tree, a non-edible oil, is used in the painting and varnish industries (Sharma and Kundu, 2006). In the literature, there are studies on the effect of tung biodiesel on engine performance and emission characteristics; to the best of the authors' knowledge, no study has been conducted on diesel engines fueled with tung biodiesel based on the second law of thermodynamics. The majority of the previous studies focused on the torque, power, and fuel consumption, which are connected to the first law of thermodynamics. The gap in existing research involves the absence of a comparison between diesel and biodiesel, concerning their impact on the irreversibility within engines, as assessed through the second law of thermodynamics. Therefore, the aim of this study was to reveal the energetic, exergetic, thermoeconomic, and exergoeconomic performances of a diesel engine fueled with tung biodiesel at high engine speeds. The study includes the following:

- Evaluating test fuels through engine test data to compare energy and exergy analyses.
- Enlightening useful work distribution and at various engine speeds.
- Examining the rates of energy and exergy losses and the irreversibilities of diesel and diesel–tung biodiesel blend.
- Determining the thermoeconomic and exergoeconomic analyses for the capital costs of diesel and diesel–tung biodiesel blend.

TABLE 1 Physicochemical properties of biodiesel from various sources.

Biodiesel	Density (kg/m^3)	Kinematic viscosity (mm^2/s)	Cetane number	Calorific value (MJ/kg)	Flash point (°C)	Cloud point (°C)	Pour point (°C)
Safflower (Kanimozhi et al. (2023))	857.8	3.97 @ 40°C	52	42.2	183	−7	-
Karanja (Kanimozhi et al. (2023))	889	5.32 @ 40°C	57	41.9	116	4	-
Eichhornia crassipes (Jain et al. (2023b))	874	3.96 @ 40°C	55	39.87	147.85	-	7
Waste cooking oil (Meng et al. (2023))	871	5.25 @ 20°C	56	39.5	-	-	-
Mahua (Jit Sarma et al. (2023))	870	-	55	39.17	148	-	-
Algae (Sharma et al. (2024))	860	-	55	39.67	421	-	-
Coconut (Lugo-Méndez et al. (2021))	860	2.352 @ 40°C	66	38.329	-	5.6	−4
Canola (Öztürk and Can. (2022))	884.4	4.526 @ 40 °C	54.3	-	177.6	−5	−12
Jatropha (Bilal Ameer et al. (2022))	870	5.25 @ 40°C	49.5	39.46	-	-	-
Roselle (Bilal Ameer et al. (2022))	877	4.65	52.1	38.75	-	-	-

2 Materials and methods

Biodiesel may be construed as methyl esters from vegetable oil through transesterification with methanol addition (Mahla et al., 2023). In this study, biodiesel was produced from tung oil via the transesterification reaction. Before the reaction, the oil is heated to 60°C while the catalyst (sodium hydroxide) dissolves inside the reactant (methanol) to prepare methoxide. After dissolving, methoxide was poured into the flask containing the heated oil. The mixture was stirred for 2 hours at a constant temperature. Following the reaction, the mixture (crude methyl ester) was transferred to a separating funnel to separate glycerin. After 8 hours, the collected methyl ester was washed three times with warm water and then dried at 105°C for 1 hour. Finally, methyl ester was filtered to remove small impurities in it.

In the experiments, a 20% (by volume) biodiesel and 80% low-sulfur diesel fuel blend was used. The properties of the pure low-sulfur diesel fuel and biodiesel blended fuel are given in Table 2. The analysis of the fuel properties was performed using the Tanaka AKV-202 Auto Kinematic Viscosity Measuring System to determine the viscosity, Zeltex ZX 440 NIR to measure the cetane number, Kyoto electronics DA-130 for density measurement, and IKA Werke C2000 bomb calorimeter to determine the heating value.

A Mitsubishi Canter 4D34-2A direct-injected diesel engine was used in the engine experiments, and the schematic representation of the experimental setup is shown in Figure 1. All experiments were performed on a four-stroke, four-cylinder, naturally aspirated, direct-injected diesel engine. Engine experiments were performed with three replicates, and the resulting averages were used for the analysis. The technical specifications of the diesel engine are detailed in Table 3. During the experiments, the engine speed reached up to 2,800 rpm, and then, the speeds were decreased to 2,600 and 2,400 rpm. In order to measure the engine torque, a hydraulic dynamometer, having a torque range of 0–1,700 Nm and speed range of 0–7,500 rpm, was coupled to the engine. For the measurement of the temperature, K-type thermocouples were used, while exhaust emission values were determined using the MRU Delta 1600 V gas analyzer, which can measure CO, CO_2, O_2, NO, and NO_2 emissions.

2.1 Energy–exergy analyses

To assess the system's productivity in terms of energy and exergy, the first and second laws of thermodynamics were applied to the engine system, which was considered the control volume. Following the approach outlined by Wang et al. (2016), the chemical reactions (Eq. 1) of the experimental fuels were established using emission data obtained from the experiments.

$$0.8aC_{14}H_{25} + 0.2aC_xH_yO_z + b(O_2 + 3.76N_2) \rightarrow cO_2 + dCO + eCO_2 + fNO + gNO_2 + hN_2 + jH_2O \quad (1)$$

In the reaction equation, all the coefficients were determined using the mass conservation equation. For the calculations, some assumptions were made to simplify the analyses. The schematic display of control volume, which encompasses the entire engine, was considered a steady-state open system, as shown in Figure 2. The intake air and exhaust gasses were assumed as ideal gas mixtures. The potential and kinetic energy of fuel, exhaust gasses, and combustion air were neglected. The pressure and temperature of the reference environment were assumed as 1 atm and 25°C, respectively.

TABLE 2 Properties of test fuels and their relevant standards.

	Diesel	B20	EN 14214	EN 590
Kinematic viscosity at 40°C (mm^2/s)	2.8	3.6	3.5–5.0	2.0–4.5
Density (kg/m^3)	833	854	860–900	820–845
Heating value (kJ/kg)	45,756	44,482	-	-
Cetane number	59.4	56.1	Min 51	Min 51

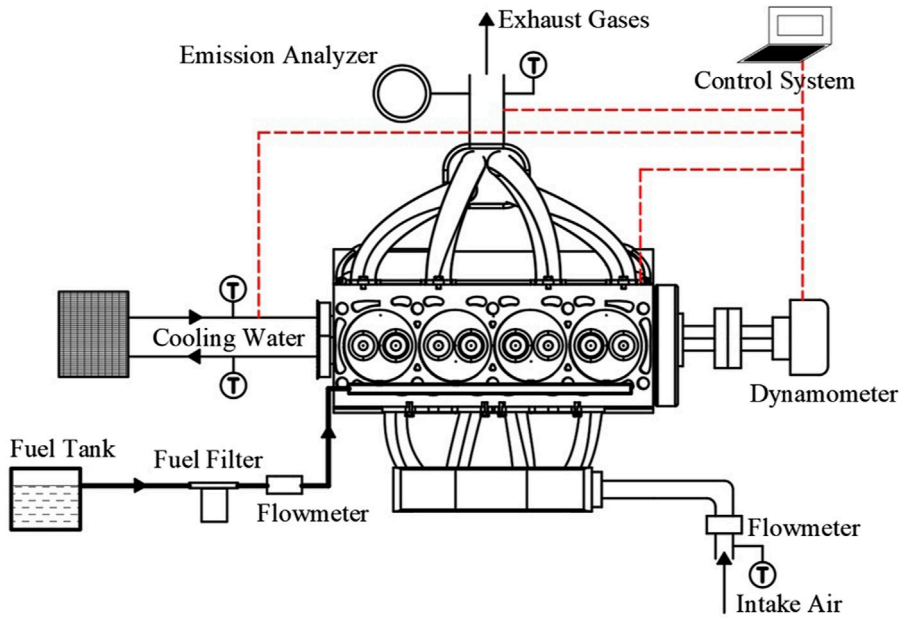

FIGURE 1
Schematic representation of the experimental setup.

The energy analysis depends on the first law of thermodynamics, which was used to determine the energy inputs and outputs of the system. On the other hand, the second law of thermodynamics is the base of the exergy analysis. Exergy can be identified as the amount of energy to obtain the net physical work. Some part of exergy leaves the control system by passing the system boundary, and some parts of exergy are destroyed due to the irreversibility of the system. Therefore, the exergy analysis is a good pathfinder to create a more effective and more durable energy system.

The approaches used during the calculations of energy and exergy analyses are given in Table 4.

2.2 Thermoeconomic–exergoeconomic analyses

In the thermoeconomic analysis of the engine system, the exergy–cost–energy–mass (EXCEM) method is employed. This method assesses the overall impact of capital investment, operational and maintenance costs, and other expenses. The equation dealing with the cost balance of the system can be demonstrated as shown in Eq. 2 (Dincer and Zamfirescu, 2016; Caliskan and Mori, 2017):

$$\Delta P = P_{in} + P_{gen,t} - P_{out} \tag{2}$$

In other words, the total cost generation can be stated as indicated in Eq. 3:

$$P_{gen,t} = P_{ci} + P_{om} + P_{oc} \tag{3}$$

Herein, $P_{gen,t}$ is the sum of the capital cost (P_{ci}), operation and maintenance costs (P_{om}), and the other costs (P_{oc}).

The majority of the total cost generation is attributed to the capital cost (P_{ci}). Therefore, instead of $P_{gen,t}$, the only capital cost of system is used during the determination of the thermoeconomic parameter (kW/$), and the thermoeconomic parameter (R_{thrm}) is given in Eq. 4 (Dincer and Rosen Marc A., 2012; Caliskan and Mori, 2017):

$$R_{thrm} = \frac{\dot{Q}_{loss}}{P_{ci}} \tag{4}$$

where $\dot{Q}_{loss}$ and P_{ci} are the energy loss rate and the capital cost of the system, respectively.

10.3389/fenrg.2024.1326466

TABLE 3 Technical specifications of the diesel engine.

Brand	Mitsubishi Canter
Model	4D34-2A
Cylinder number	Four in-line
Engine type	Four-stroke, natural aspirated
Displacement	3907 cc
Maximum power	89 kW at 3,200 rpm
Maximum torque	295 Nm at 1,800 rpm
Stroke × bore	115 mm × 104 mm

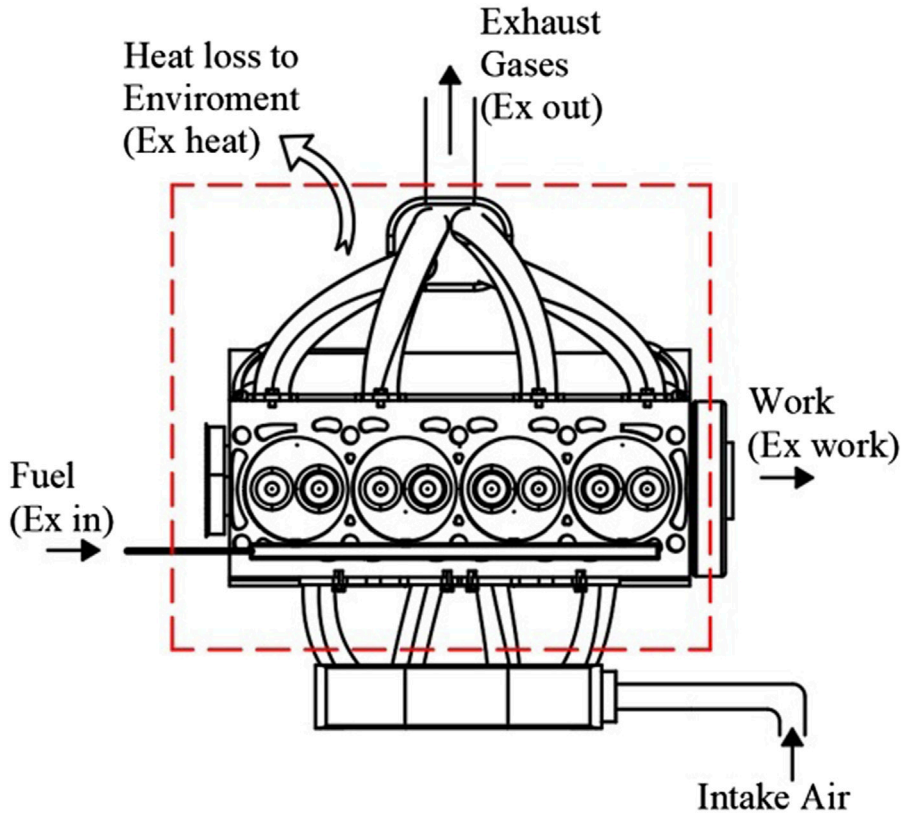

FIGURE 2
Schematic display of the control volume of the engine.

When the energy analysis is synthesized with the economic analysis, the exergoeconomic parameter is obtained. The EXCEM method underlies the description of the exergoeconomic parameter (R_{exg}), and it is indicated in Eq. 5:

$$R_{exg} = R_{ex,lth} + R_{ex,des} \tag{5}$$

$$R_{ex,lth} = \frac{\dot{E}_{x,heat}}{P} \tag{6}$$

$$R_{ex,des} = \frac{\dot{E}_{x,dest}}{P} \tag{7}$$

It is seen that R_{exg} includes the parameter of exergy loss through heat transfer ($R_{ex,lth}$), along with the parameter of exergy destruction ($R_{ex,des}$), which are presented in Eqs 6, 7, respectively. Here, $\dot{E}_{x,dest}$ and $\dot{E}_{x,heat}$ are the exergy destruction rate and the exergy heat loss rate, respectively.

3 Results and discussion

3.1 Energy analysis

In this study, the effects of adding 20% (by volume) of tung biodiesel into diesel fuel were examined at high engine speeds (2,400,

10.3389/fenrg.2024.1326466

TABLE 4 Equations of energy and exergy analyses.

Model	Equation
Model balance equation	$\sum \dot{m} = \sum \dot{m}_{out}$
Energy balance equation	$\sum \dot{E} = \sum \dot{E}_{out}$, $\dot{Q} - W = \sum \dot{m}_{out} h_{out} - \sum 5$
Work rate	W = ωT
Energy input	$\dot{E}_{fuel} = \dot{m}_{fuel} H_u$
Energy heat loss	$\dot{Q}_{loss} = \dot{E}_{fuel} - (W + \dot{Q}_{exh})$
Exhaust energy	$\dot{Q}_{exh} = \sum \dot{m}_{out} \Delta h_{out}$
Energy efficiency	$\eta t = \frac{\dot{W}}{\dot{E}_{fuel}}$
Exergy balance equation	$\sum \dot{E}x_i = \dot{E}x_{out} + \dot{E}x_{heat} + \dot{E}x_{work} + \dot{E}x_{dest}$
Exergy input	$\dot{E}x_i = \dot{m}_{fuel} \varepsilon_{fuel}$
Specific exergy of fuel	$\varepsilon_{fuel} = \overline{LHV}_{fuel} \varphi$
Chemical exergy factor	$\varphi = 1.0401 + 0.1728 \frac{h}{c} + 0.0432 \frac{o}{c} + 0.2169 \frac{e}{c} (1 - 2.0628 \frac{h}{c})$
Exhaust exergy	$\dot{E}x_{out} = \sum \dot{m}_i (\varepsilon_{tm} + \varepsilon_{chem})_i$
Thermo-mechanical exergy	$\varepsilon_{tm} = (h - h_o) - T_o (s - s_o)$
Chemical exergy	$\varepsilon_{chem} = \bar{R} T_o \, ln \frac{y_i}{y_r}$
Exergy heat loss	$\dot{E}x_{heat} = \sum (1 - \frac{T_0}{T_{cw}}) \dot{Q}_{loss}$
Exergy efficiency	$\psi = \frac{\dot{E}x_{work}}{\dot{E}x}$
Entropy generation	$S_{EG} = \frac{\dot{E}x_{dest}}{T_0}$

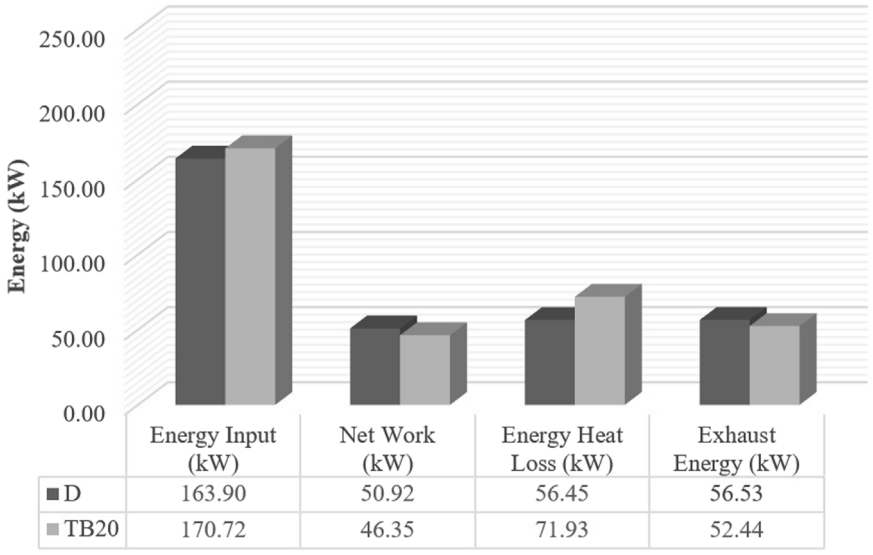

FIGURE 3
Energy distribution for diesel fuel and DTB20 fuel at the engine speed of 2,400 rpm.

2,600, and 2,800 rpm). The results of the energy–exergy analyses of conventional diesel fuel and the diesel–tung biodiesel blend (DTB20) were compared to assess the impact of tung biodiesel addition. The energy distributions of the engine system at different speeds (2,400, 2,600, and 2,800 rpm) are displayed in Figures 3–5, respectively. At the engine speed of 2,400 rpm, as shown in Figure 3,

10.3389/fenrg.2024.1326466

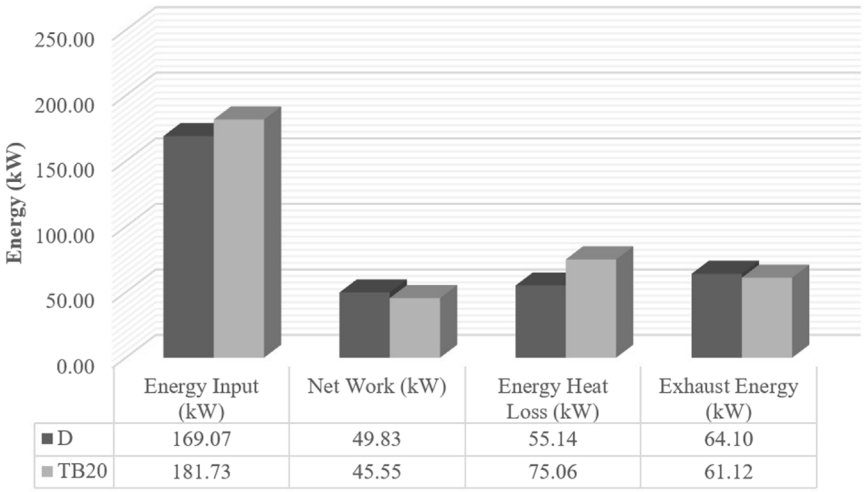

FIGURE 4
Energy distribution for diesel fuel and DTB20 fuel at the engine speed of 2,600 rpm.

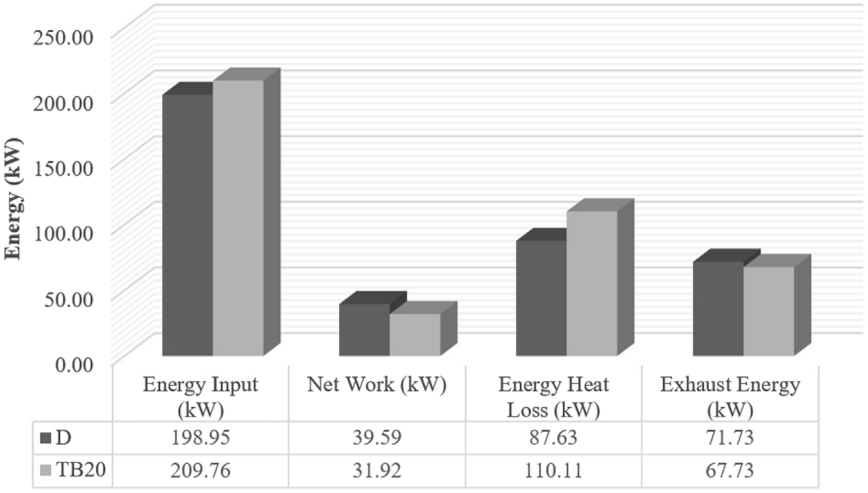

FIGURE 5
Energy distribution for diesel fuel and DTB20 fuel at the engine speed of 2,800 rpm.

the fuel energy obtained from the diesel–tung biodiesel blend was greater than that obtained from conventional diesel fuel. However, the energy converted into useful work for the diesel–tung biodiesel blend fuel was lower than that for conventional diesel fuel. A total of 31.07% of the input fuel energy of diesel fuel was converted to useful work, while only 27.15% of the input fuel energy of DTB20 fuel was converted into useful work.

At the engine speeds of 2,600 and 2,800 rpm, the variation in the fuel input energy exhibited a similarity with the case of 2,400 rpm. The fuel energy values of DTB20 fuels were significantly higher than those of pure diesel fuels. Additionally, the fuel energy derived from all tests increased as the engine speed increased due to the distinct rise in the fuel mass flow rate. In terms of energy conservation to useful work, the trend of variation was the opposite of the input fuel energy variation. The amount of useful work decreased significantly as the engine speed increased. A noticeable reduction in the amount of useful work compared to that of case of 2,400 rpm was observed, especially for the engine speed of 2,800 rpm, owing to the increment of friction forces between the engine components. Moreover, the useful work of the engine fueled with DTB20 fuels at 2,600 rpm and 2,800 rpm was lower than that of the corresponding cases of the engine operated with pure diesel fuel, as observed in the 2,400-rpm case.

A major portion of heat energy generated during the combustion in the engine system was dissipated through cooling water, which is referred to as the energy heat loss in the energy analyses. It can be observed from Figures 3–5 that the energy heat losses of DTB20 fuels at all engine speeds were significantly higher than those of the conventional diesel fuels. The energy heat loss rates for pure diesel and DTB20 fuels were determined as 34.44% and

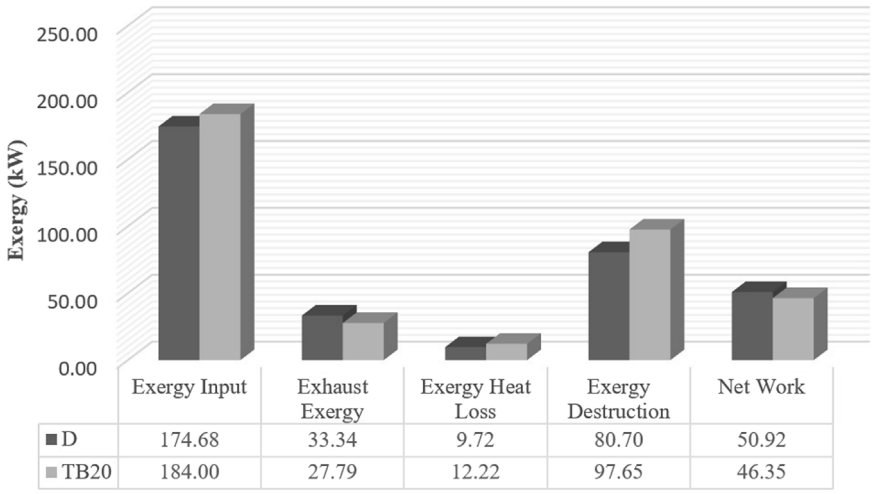

FIGURE 6
Exergy distribution for diesel fuel and TB20 fuel at the engine speed of 2,400 rpm.

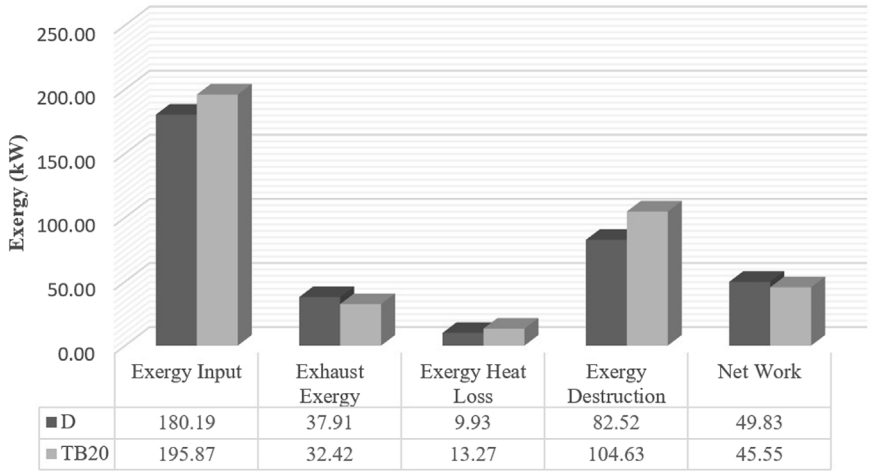

FIGURE 7
Exergy distribution for diesel fuel and TB20 fuel at the engine speed of 2,600 rpm.

42.13%, respectively. These corresponding energy heat loss rates rise up to 44.05% and 52.49%, respectively, as the engine reached 2,800 rpm with regard to the enhancement of the outlet temperature of cooling water.

Another substantial portion of the input fuel energy is carried away by exhaust gases, herein referred to as the exhaust energy rate. The experimental results indicated that the energy moved away as the exhaust gases increased with the engine speed, both for diesel fuel and DTB20 fuel, owing to the rise in fuel consumption and the exhaust gas temperature. The exhaust energy rates of diesel fuels at the engine speeds of 2,400, 2,600, and 2,800 rpm were determined as 34.49%, 37.91%, and 36.05%, respectively, while for DTB20 fuels, these rates were assessed as 30.72%, 33.63%, and 32.29%, respectively. Notably, the exhaust energy rates of DTB20 fuels were consistently lower than those of pure diesel fuels at all engine speeds since the temperature of exhaust gases when using DTB20 fuels was less than that when using conventional diesel fuels.

3.2 Exergy analysis

The main aim of conducting exergy analysis is to reveal the interaction among consumption, environmental effects, energy generation, and system irreversibilities (Aghbashlo et al., 2017). Exergy analyses were carried out for the diesel engine fueled with conventional diesel fuel and DTB20 fuel at three distinct high engine speeds of 2,400, 2,600, and 2,800 rpm. The findings of the exergy analysis are depicted in Figures 6–8 for 2,400, 2,600, and 2,800 rpm, respectively. At 2,400 rpm, as indicated in Figure 6, 29.15% of the input exergy was utilized for useful work, 5.56% of that was transferred to cooling water through heat transfer, 19.09% was

10.3389/fenrg.2024.1326466

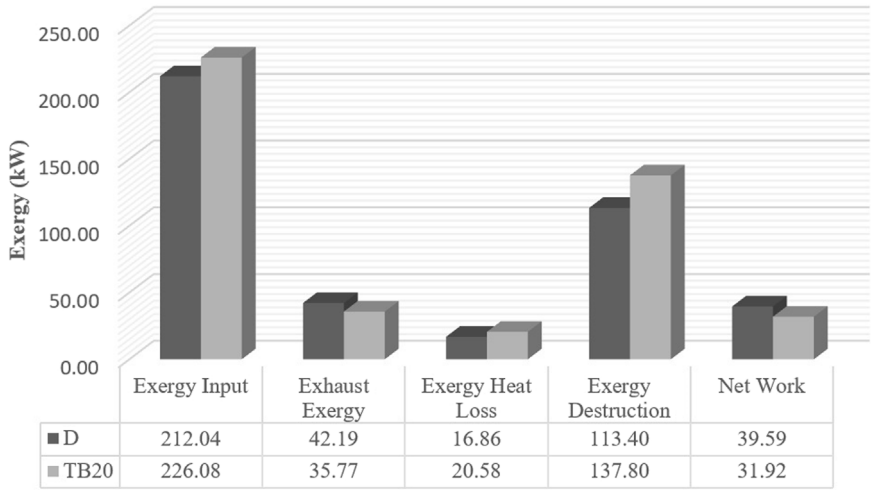

FIGURE 8
Exergy distribution for diesel fuel and TB20 fuel at the engine speed of 2,800 rpm.

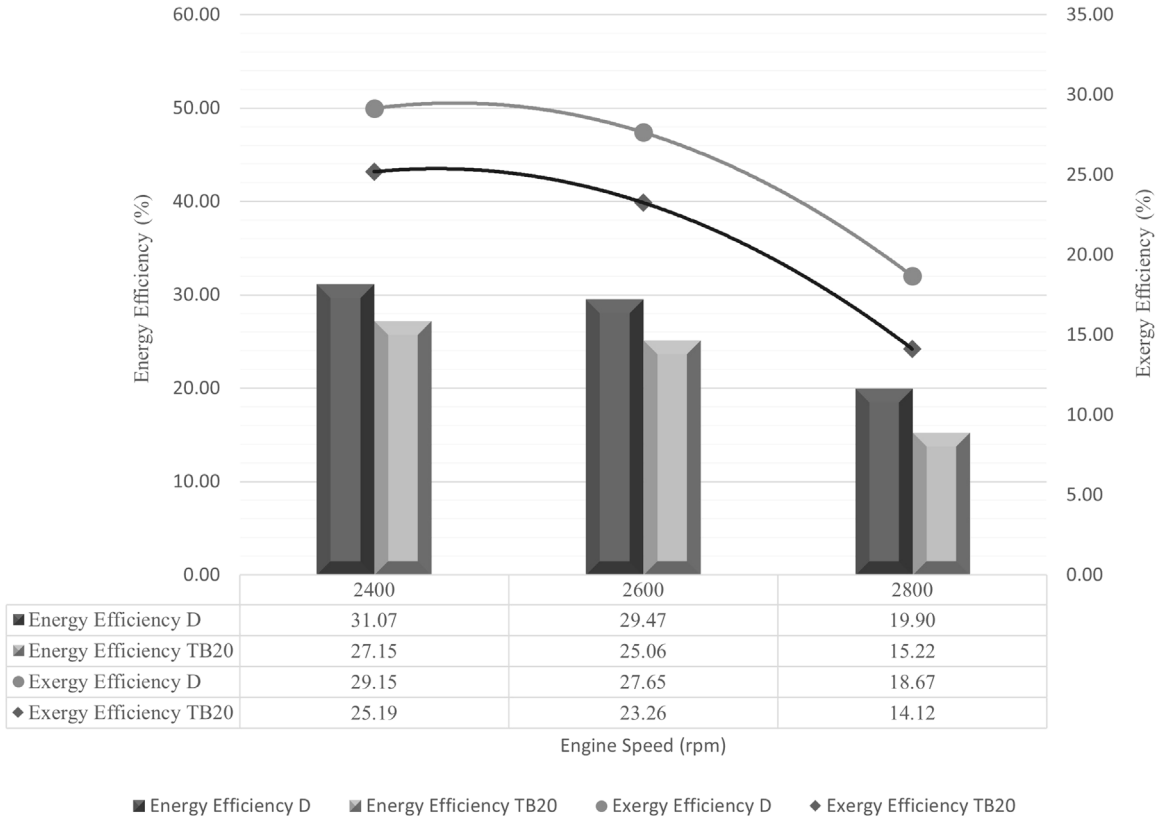

FIGURE 9
Variation in the energy–exergy efficiencies versus the engine speed for the diesel engine operated with diesel fuel and DTB20 fuel.

expelled by the exhaust gases, and the remaining 46.20% of the input exergy was destroyed within the engine system when fueled with pure diesel. In the case of the DTB20 fuel, the exergy distribution trend showed a quite similar trend with that of diesel fuels. The input exergy conservation rate to the exergy work and the exergy heat loss were determined as 25.19% and 6.64%, respectively. The exergy destruction rate was found to be approximately 53.07%, which was more than half of the input exergy, while the exhaust energy rate was 15.10%. These findings proved that the exergy destruction rate and the exhaust exergy rate of the DTB20 fuel were higher than those of

TABLE 5 Comparison of the performance in terms of energy–exergy analyses with the other studies in the literature.

Used fuel	Energy efficiency	Exergy efficiency	Authors of studies
Diesel (D100)	31.92	29.77	Sarıkoç et al. (2020)
Diesel–biodiesel–butanol (D60B20But20)	30.17	28.13	
SMB0 (0% spirulina biodiesel + 100% diesel)	33.55	31.48	Rajpoot et al. (2023)
SMB100 (0% spirulina biodiesel +100% diesel)	31.89	29.51	
Diesel	33.5	31.4	Gozmen Şanli et al. (2019)
OPB	32.3	30	
PB	32.1	29.85	
D100 (diesel)	28.23	20	Dogan et al. (2022)
F5 (5% fusel oil + 95% diesel)	28	20.68	
F10 (105% fusel oil + 90% diesel)	27.9	19.87	
F20 (20% fusel oil + 80% diesel)	26.09	19	
F30 (30% fusel oil + 70% diesel)	24.93	18.05	
Mixture of waste cooking oil/canola oil (50:50 v/v) biodiesel	22.13	20.05	Yeşilyurt and Arslan (2019)
Diesel	19.90–31.07	18.67–29.15	Present study
DTB20 (20% tung oil biodiesel + 80% diesel)	15.22–27.15	14.12–25.19	

the diesel fuel because system irreversibilities in the engine fueled with the DTB20 fuel were higher than those for diesel fuel. Additionally, the exergy loss through heat transfer for DTB20 fuel was higher than that of diesel fuel, owing to the higher oxygen content in biodiesel fuels (Madheshiya and Vedrtnam, 2018; Gozmen Şanli et al., 2019).

Engine speed is another crucial parameter in exergy analyses. The maximum input exergy was obtained at the engine speed of 2,800 rpm for both diesel and DTB20 fuels. However, the highest exergy converted into useful work was achieved with diesel fuel at 2,400 rpm, due to higher friction forces occurring between the engine components at higher engine speeds. As the engine speed increased, the net work rate significantly diminished for all tested fuels due to the significant increment in the fuel consumption rate and the decrease in the net work rate at the engine speed of 2,800 rpm, which was evident nearly as 10.48% for diesel fuel and 11.07% for DTB20 fuel compared to those of the case of 2,400 rpm. Regarding exhaust exergy, the increase in the engine speed led to a higher exergy being carried away by exhaust gases. This was a result of the elevated exhaust gas temperature and increased fuel consumption for all tested fuels.

For all test fuels, the exergy destruction and exergy heat loss rose with the increase in engine speed since friction on the engine components augmented with the enhancement of the engine speed. Moreover, for all engine speeds, the findings for DTB20 fuel exhibited that the values of exergy destruction and exergy heat loss were significantly higher than those of diesel fuel. This can be attributed to the higher oxygen content in biodiesel fuels, leading to a more efficient combustion. Consequently, both exergy loss through cooling water and the temperature inside the cylinder increased.

The variations in the energy efficiency and the exergy efficiency, as a function of engine speed for both diesel and DTB20 fuels, are demonstrated in Figure 9. The variations in the energy efficiency and the exergy efficiency showed a similar trend. At the engine speed of 2,400 rpm, the energy efficiency of the engine fueled with diesel was approximately 31.07%, and the exergy efficiency was calculated as 29.15%, while the energy efficiency of the engine fueled with TB20 fuel was assessed as 27.15%, and the exergy efficiency was approximately 25.19%. The maximum energy efficiency and exergy efficiency for all test fuels were achieved at 2,400 rpm. As the engine speed increased, both the energy efficiency and exergy efficiency decreased for all tested fuels, due to the rise in mechanical friction within the engine. At 2,800 rpm, the energy efficiency and exergy efficiency of diesel fuel decreased to 19.90% and 18.67%, respectively, while the corresponding efficiency values of DTB20 fuels were 15.22% and 14.12%, respectively. Moreover, for all engine speeds, the energy efficiency of the engine operated with diesel fuel was higher than that of DTB20 fuel, owing to a higher cetane number of diesel fuel in comparison to that of DTB20 fuel. Hürdoğan (2016) defined the cetane number as a significant parameter corresponding with the increment of the combustion quality during the ignition process of the diesel engines. In terms of comparing the energy efficiency and the exergy efficiency, the exergy efficiency was lower than the energy efficiency for all fuels since a significant amount of exergy destruction occurred during fuel combustion, and only a small amount of fuel input exergy can be converted into the work exergy (Aghbashlo et al., 2016). When the studies in the literature were examined, it can be concluded that the findings deal with both the energy efficiency and exergy efficiency and the variation in the trends of energy–exergy efficiencies that coincide

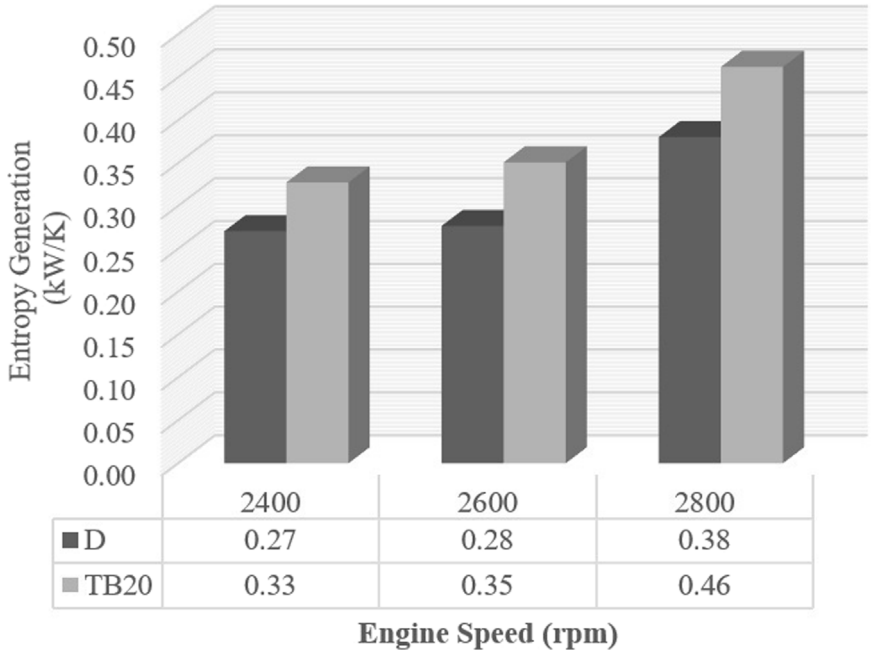

FIGURE 10
Entropy generation of the diesel engine operated with diesel fuel and DTB20 fuel as a function of the engine speed.

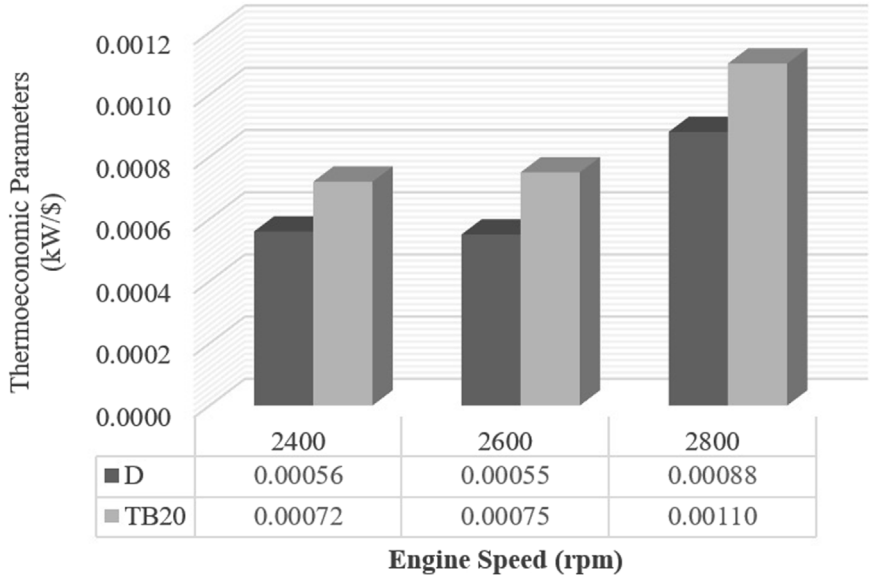

FIGURE 11
Thermoeconomic parameters of the diesel engine operated with diesel fuel and DTB20 fuel as a function of the engine speed.

with the findings of many studies in the literature, as given in Table 5.

To analyze the thermodynamics of the irreversibilities of thermal machines, such as heat pumps, refrigerators, and engines, the entropy generation parameter is defined. Figure 10 depicts the variation in the entropy generation of the diesel engine with respect to the engine speed. At the engine speed of 2,400 rpm, the entropy production of the system for the diesel fuel was assessed as 0.27 kW/K, while the entropy generation of the system for the DTB20 fuel was 0.33 kW/K, with regard to the equations. As the engine's speed increased, the entropy production rates augmented for all fuel types since the enhancement of the engine speed leads to a higher fuel consumption rate and higher cylinder wall temperatures, which, in turn, enhanced entropy generation through heat transfer to the environment and the coolant. When the effect of the fuel type on exergy destruction was investigated, it was deduced that the

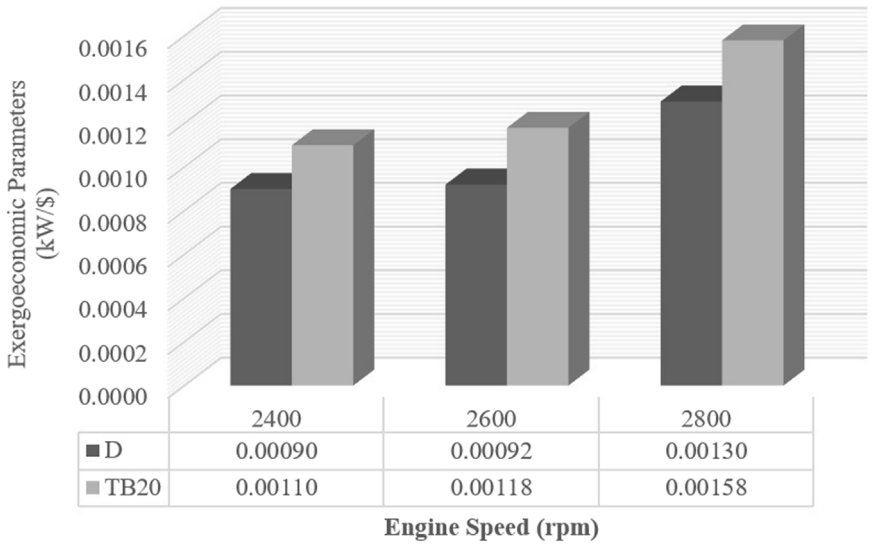

FIGURE 12
Exergoeconomic parameters of the diesel engine operated with diesel fuel and DTB20 fuel as a function of the engine speed.

entropy production of the engine fueled with the DTB20 fuel was higher than that of the diesel fuel at all engine speeds. This is due to the higher exergy destruction in the engine fueled with the DTB20 fuel compared to the engine fueled with the diesel fuel.

3.3 Thermoeconomic analysis

The results of thermoeconomic analyses are presented in Figure 11. To gather information about the energy heat loss per capital cost, it is essential to consider the cost incurred by the energy heat loss in the engine system, which is treated as an additional cost. At 2,400 and 2,600 rpm, the thermoeconomic parameters for the engine operating with diesel fuel were determined as 0.00056 and 0.00055, respectively. However, the thermoeconomic parameter increased to 0.00088 when the engine accelerated to 2,800 rpm, due to the increased heat loss. For the engine fueled with DTB20 fuel, the trend of thermoeconomic parameters with the engine speed was similar to that of the diesel fuel usage. At all engine speeds, the value of the thermoeconomic parameter obtained with the usage of the DTB20 fuel was higher than that of the diesel fuel usage.

3.4 Exergoeconomic analysis

The exergoeconomic parameter is defined as the summation of the exergy heat loss per capital cost and the exergy destruction per capital cost. This parameter assesses the impact of total exergy losses on the cost of the engine system. The results of the exergoeconomic analysis can be used to optimize the exergy losses and minimize it [Caliskan and Mori, 2017]. Figure 12 indicates the variation in the exergoeconomic parameter with the engine speed. The trend of the exergoeconomic parameter's variation with the engine speed was similar and coincided with the findings of the thermoeconomic analysis for all experimental fuels. For both diesel fuel and DTB20 fuel, there was almost no difference between the value of the exergoeconomic parameter for the case of 2,400 and 2,600 rpm. However, as the thermoeconomic parameters, the value of the exergoeconomic parameter at the engine speed of 2,800 rpm augmented significantly compared to the other engine speeds for all fuels due to higher friction inducing mechanical losses. Moreover, in terms of the fuel type, it can be concluded that the use of diesel fuel was preferable compared to the DTB20 fuel regarding an exergoeconomic evaluation.

4 Conclusion

The current study focused on the energetic–exergetic, thermoeconomic, and exergoeconomic analyses of a diesel engine fueled with diesel fuel and the diesel–tung biodiesel (20%, by volume) blend (DTB20 fuel) at high engine speeds (2,400, 2,600, and 2,800 rpm). The key findings of this study can be listed as follows:

- The findings revealed that the amount of energy converted to useful work with the conventional diesel fuel was higher than that of the DTB20 fuel, even though the fuel energy obtained from the DTB20 fuel was higher than that of the diesel fuel at all engine speeds.
- The highest energy efficiency and exergy efficiency were obtained at the engine speed of 2,400 rpm for both diesel and the DTB20 fuel. The energy and exergy efficiencies of the engine fueled with diesel fuel were obtained as 31.07% and 29.15%, respectively, while the corresponding values for the engine fueled with the DTB20 fuel were determined as 27.15% and 25.19%, respectively.
- With the acceleration of the engine to 2,800 rpm, a significant decrease in both the energy and exergy efficiencies was observed for both diesel fuel and DTB20 fuel due to the enhancement of mechanical friction in the engine.

- The entropy generation parameter increased with the increase in the engine speed. At the engine speed of 2,400 rpm, entropy generation was assessed as being 0.27 kW/K for the case of diesel fuel and 0.33 kW/K for the case of DTB20 fuel. At 2,800 rpm, entropy generation increased to 0.38 kW/K for diesel fuel and 0.46 kW/K for DTB20 fuel since the enhancement of the engine speed caused the ascent of the fuel consumption rate and the temperature of the cylinder wall.
- With regard to thermoeconomic and exergoeconomic evaluations, diesel fuel is better compared to DTB20 fuel. For both diesel fuel and DTB20 fuel, the values of thermoeconomic–exergoeconomic parameters showed a similarity with the corresponding case at the engine speed of 2,400 and 2,600 rpm. However, the values of thermoeconomic–exergoeconomic parameters at the engine speed of 2,800 rpm augmented significantly compared to the values obtained at other engine speeds due to the enhancement of friction inducing the mechanical losses.

All the findings of the present study indicate that diesel fuel outperforms TB20 fuel in terms of the second law of thermodynamics. This study also highlights the fact that the critical engine speed is 2,600 rpm. Beyond this threshold, the engine system was found to operate inefficiently, according to the second law of thermodynamics and per capita costs.

Data availability statement

The original contributions presented in the study are included in the article/Supplementary Material; further inquiries can be directed to the corresponding author.

Author contributions

BS: formal analysis, investigation, methodology, writing–original draft, and writing–review and editing. OG: investigation, methodology, writing–original draft, and writing–review and editing. MÖ: supervision, writing–original draft, and writing–review and editing. EU: supervision, writing–original draft, and writing–review and editing.

Funding

The author(s) declare that no financial support was received for the research, authorship, and/or publication of this article.

Conflict of interest

The authors declare that the research was conducted in the absence of any commercial or financial relationships that could be construed as a potential conflict of interest.

Publisher's note

All claims expressed in this article are solely those of the authors and do not necessarily represent those of their affiliated organizations, or those of the publisher, the editors, and the reviewers. Any product that may be evaluated in this article, or claim that may be made by its manufacturer, is not guaranteed or endorsed by the publisher.

References

Aghbashlo, M., Tabatabaei, M., Khalife, E., Najafi, B., Mirsalim, S. M., Gharehghani, A., et al. (2017). A novel emulsion fuel containing aqueous nano cerium oxide additive in diesel–biodiesel blends to improve diesel engines performance and reduce exhaust emissions: Part II – exergetic analysis. *Fuel* 205, 262–271. doi:10.1016/j.fuel.2017.05.003

Aghbashlo, M., Tabatabaei, M., Mohammadi, P., Mirzajanzadeh, M., Ardjmand, M., and Rashidi, A. (2016). Effect of an emission-reducing soluble hybrid nanocatalyst in diesel/biodiesel blends on exergetic performance of a DI diesel engine. *Renew. Energy* 93, 353–368. doi:10.1016/j.renene.2016.02.077

Aslan, V. (2023). Fuel characterization, engine performance characteristics and emissions analysis of different mustard seed biodiesel: an overview. *J. Biotechnol.* 370, 12–30. doi:10.1016/j.jbiotec.2023.05.006

Bilal Ameer, H. M., Ameer, M. F., Ghachem, K., Ali, M., Razaq, A., Khan, S. U., et al. (2022). Experimental comparison of performance and emission characteristics of 4-stroke CI engine operated with Roselle and Jatropha biodiesel blends. *J. Indian Chem. Soc.* 99, 100505. doi:10.1016/j.jics.2022.100505

Caliskan, H., and Mori, K. (2017). Thermodynamic, environmental and economic effects of diesel and biodiesel fuels on exhaust emissions and nano-particles of a diesel engine. *Transp. Res. Part D. Transp. Environ.* 56, 203–221. doi:10.1016/j.trd.2017.08.009

Cavalcanti, E. J. C., Carvalho, M., and Ochoa, A. A. V. (2019). Exergoeconomic and exergoenvironmental comparison of diesel-biodiesel blends in a direct injection engine at variable loads. *Energy Convers. Manag.* 183, 450–461. doi:10.1016/j.enconman.2018.12.113

Celebi, K., Uludamar, E., and Özcanlı, M. (2017). Evaluation of fuel consumption and vibration characteristic of a compression ignition engine fuelled with high viscosity biodiesel and hydrogen addition. *Int. J. Hydrogen Energy* 42, 23379–23388. doi:10.1016/j.ijhydene.2017.02.066

Dincer, I., and Rosen Marc, A. (2012). *Exergy energy, environment and sustainable development*. Elsevier Science.

Dincer, I., and Zamfirescu, C. (2016). *Sustainable hydrogen production*. Elsevier Science.

Dogan, B., Özer, S., and Erol, D. (2022). Exergy, exergoeconomic, and exergoenvironmental evaluations of the use of diesel/fusel oil blends in compression ignition engines. *Sustain. Energy Technol. Assessments* 53, 102475. doi:10.1016/j.seta.2022.102475

El-adawy, M. (2023). Effects of diesel-biodiesel fuel blends doped with zinc oxide nanoparticles on performance and combustion attributes of a diesel engine. *Alex. Eng. J.* 80, 269–281. doi:10.1016/j.aej.2023.08.060

Goga, G., Singla, V., Mahla, S. K., Chauhan, B. S., Dhir, A., Balasubramaniam, D., et al. (2021). Effects of ternary fuel blends (diesel-biodiesel-n-butanol) on emission and performance characteristics of diesel engine using varying mass flow rates of biogas. *Energy Source. Part A*, 1–14. in press. doi:10.1080/15567036.2021.1910754

Goyal, D., Goyal, T., Mahla, S. K., Goga, G., Dhir, A., Balasubramanian, D., et al. (2023). Application of Taguchi design in optimization of performance and emissions characteristics of n-butanol/diesel/biogas under dual fuel mode. *Fuel* 338, 127246. doi:10.1016/j.fuel.2022.127246

Gozmen Şanli, B., Uludamar, E., and Özcanli, M. (2019). Evaluation of energetic-exergetic and sustainability parameters of biodiesel fuels produced from palm oil and opium poppy oil as alternative fuels in diesel engines. *Fuel* 258, 116116. doi:10.1016/j.fuel.2019.116116

Harish, H., Rajanna, S., Prakash, G. S., and Ahamed, S. M. (2019). Extraction of biodiesel from tung seed oil and evaluating the performance and emission studies on 4-stroke CI engine. *Mat. Today Proc.* 46, 4869–4877. doi:10.1016/j.matpr.2020.10.328

Hürdoğan, E. (2016). Thermodynamic analysis of a diesel engine fueled with diesel and peanut biodiesel. *Environ. Prog. Sustain. Energy* 35, 891–897. doi:10.1002/ep.12268

Jain, A., Jyoti, B., Kumar, R., Sharma, P., Jyoti, B., Venkata, G., et al. (2023a). Energy, exergy and emission [3E] analysis of Mesua Ferrea seed oil biodiesel fueled diesel engine at variable injection timings. *Fuel* 353, 129115. doi:10.1016/j.fuel.2023.129115

Jain, A., Jyoti Bora, B., Kumar, R., Sharma, P., Jyoti Medhi, B., Ahsan Farooque, A., et al. (2023b). Impact of titanium dioxide (TiO2) nanoparticles addition in Eichhornia Crassipes biodiesel used to fuel compression ignition engine at variable injection pressure. *Case Stud. Therm. Eng.* 49, 103295. doi:10.1016/j.csite.2023.103295

Jit Sarma, C., Sharma, P., Bora, B. J., Bora, D. K., Senthilkumar, N., Balakrishnan, D., et al. (2023). Improving the combustion and emission performance of a diesel engine powered with mahua biodiesel and TiO2 nanoparticles additive. *Alex. Eng. J.* 72, 387–398. doi:10.1016/j.aej.2023.03.070

Kanimozhi, B., Karthikeyan, L., Praveenkumar, T. R., Ali Alharbi, S., Alfarraj, S., and Gavurová, B. (2023). Evaluation of karanja and safflower biodiesel on engine's performance and emission characteristics along with nanoparticles in DI engine. *Fuel* 352, 129101. doi:10.1016/j.fuel.2023.129101

Kukana, R., and Jakhar, O. P. (2022). Performance, combustion and emission characteristics of a diesel engine using composite biodiesel from waste cooking oil - Hibiscus Cannabinus oil. *J. Clean. Prod.* 372, 133503. doi:10.1016/j.jclepro.2022.133503

Kumar, P., Kumar, D., Shankar, R., Kumar, S., Saini, P., and Kumar, N. (2023). Effect of synthesized lemongrass biodiesel on the performance and emission characteristics of a CI engine. *Sustain. Energy Technol. Assessments* 57, 103221. doi:10.1016/j.seta.2023.103221

Kumar, S., and Gautam, R. (2023). Energy and exergy assessment of diesel-tallow biodiesel blend in compression ignition engine for engine design variables. *Sustain. Energy Technol. Assessments* 57, 103305. doi:10.1016/j.seta.2023.103305

Li, J., Zhong, W., Zhang, J., Zhao, Z., and Hu, J. (2023). The combustion and emission improvements for diesel–biodiesel hybrid engines based on response surface methodology. *Front. Energy Res.* 11, 1–16. doi:10.3389/fenrg.2023.1201815

Liu, J., Zhang, X., Tang, C., Wang, L., Sun, P., and Wang, P. (2023). Effects of palm oil biodiesel addition on exhaust emissions and particle physicochemical characteristics of a common-rail diesel engine. *Fuel Process. Technol.* 241, 107606. doi:10.1016/j.fuproc.2022.107606

Lugo-Méndez, H., Sánchez-Domínguez, M., Sales-Cruz, M., Olivares-Hernández, R., Lugo-Leyte, R., and Torres-Aldaco, A. (2021). Synthesis of biodiesel from coconut oil and characterization of its blends. *Fuel* 295, 120595. doi:10.1016/j.fuel.2021.120595

Madheshiya, A. K., and Vedrtnam, A. (2018). Energy-exergy analysis of biodiesel fuels produced from waste cooking oil and mustard oil. *Fuel* 214, 386–408. doi:10.1016/j.fuel.2017.11.060

Mahla, S. K., Goga, G., Cho, H. M., Dhir, A., and Chauhan, B. S. (2023). Separate effect of biodiesel, n-butanol, and biogas on performance and emission characteristics of diesel engine: a review. *Biomass Convers. Biorefinery* 13, 447–469. doi:10.1007/s13399-020-01056-7

Meng, J., Xu, W., Meng, F., Wang, B., Zhao, P., Wang, Z., et al. (2023). Effects of waste cooking oil biodiesel addition on combustion, regulated and unregulated emission characteristics of common-rail diesel engine. *Process Saf. Environ. Prot.* 178, 1094–1106. doi:10.1016/j.psep.2023.08.065

Muhammed Niyas, M., and Shaija, A. (2022). Effect of repeated heating of coconut, sunflower, and palm oils on their fatty acid profiles, biodiesel properties and performance, combustion, and emission, characteristics of a diesel engine fueled with their biodiesel blends. *Fuel* 328, 125242. doi:10.1016/j.fuel.2022.125242

Nabi, M. N., Rasul, M. G., Anwar, M., and Mullins, B. J. (2019). Energy, exergy, performance, emission and combustion characteristics of diesel engine using new series of non-edible biodiesels. *Renew. Energy* 140, 647–657. doi:10.1016/j.renene.2019.03.066

Odibi, C., Babaie, M., Zare, A., Nabi, M. N., Bodisco, T. A., and Brown, R. J. (2019). Exergy analysis of a diesel engine with waste cooking biodiesel and triacetin. *Energy Convers. Manag.* 198, 111912. doi:10.1016/j.enconman.2019.111912

Öztürk, E., and Can, Ö. (2022). Effects of EGR, injection retardation and ethanol addition on combustion, performance and emissions of a DI diesel engine fueled with canola biodiesel/diesel fuel blend. *Energy* 244, 123129. doi:10.1016/j.energy.2022.123129

Raj Bukkarapu, K., and Krishnasamy, A. (2023). Support vector regression approach to optimize the biodiesel composition for improved engine performance and lower exhaust emissions. *Fuel* 348, 128604. doi:10.1016/j.fuel.2023.128604

Rajpoot, A. S., Choudhary, T., Chelladurai, H., Nath Verma, T., and Pugazhendhi, A. (2023). Sustainability analysis of spirulina biodiesel and their blends on a diesel engine with energy, exergy and emission (3E's) parameters. *Fuel* 349, 128637. doi:10.1016/j.fuel.2023.128637

Rawat, J. S., Bhowmik, S., Panua, R., Madane, P. A., and Triveni, M. K. (2023). Investigation of performance, emission and exergy parameters of a compression ignition engine fuelled with ethanol-jatropha biodiesel blend under varying hydrogen strategies. *Int. J. Hydrogen Energy* 48, 37415–37426. doi:10.1016/j.ijhydene.2023.06.128

Sarıkoç, S., Örs, I., and Ünalan, S. (2020). An experimental study on energy-exergy analysis and sustainability index in a diesel engine with direct injection diesel-biodiesel-butanol fuel blends. *Fuel* 268, 117321. doi:10.1016/j.fuel.2020.117321

Sharma, P., Mohite, A., Jyoti, B., Ümit, A., Jyoti, B., and Barik, D. (2024). Optimization of the pilot fuel injection and engine load for an algae biodiesel - hydrogen run dual fuel diesel engine using response surface methodology, *Fuel* 357. doi:10.1016/j.fuel.2023.129841

Sharma, V., and Kundu, P. P. (2006). Addition polymers from natural oils-A review. *Prog. Polym. Sci.* 31, 983–1008. doi:10.1016/j.progpolymsci.2006.09.003

Suzuki, T., Sumimoto, K., Fukada, K., and Katayama, T. (2021). Iodine value of tung biodiesel fuel using Wijs method is significantly lower than calculated value. *J. Wood Sci.* 67, 55. doi:10.1186/s10086-021-01987-3

Wang, T., Liu, T., Wang, Z., Tian, X., Yang, Y., Guo, M., et al. (2016). A rapid and accurate quantification method for real-time dynamic analysis of cellular lipids during microalgal fermentation processes in Chlorella protothecoides with low field nuclear magnetic resonance. *J. Microbiol. Methods* 124, 13–20. doi:10.1016/j.mimet.2016.03.003

Xu, L., Xu, S., Lu, X., Jia, M., and Bai, X. S. (2023). Large eddy simulation of spray and combustion characteristics of biodiesel and biodiesel/butanol blend fuels in internal combustion engines. *Appl. Energy Combust. Sci.* 16, 100197. doi:10.1016/j.jaecs.2023.100197

Yeşilyurt, M. K., and Arslan, M. (2019). Analysis of the fuel injection pressure effects on energy and exergy efficiencies of a diesel engine operating with biodiesel. *Biofuels* 10, 643–655. doi:10.1080/17597269.2018.1489674

10.3389/fenrg.2024.1326466

Nomenclature

$\dot{m}$	Mass flow rate (kg/s)
$\dot{E}$	Energy rate (kW)
$\dot{W}$	Power (kW)
ω	Angular velocity (rad/s)
T	Torque (Nm)
$\dot{Q}$	Heat rate (kW)
h	Enthalpy (kJ/kg)
S_{EG}	Entropy generation (kW/K)
T	Temperature (K)
$\dot{E}x$	Exergy rate (kW)
ε_{fuel}	Specific exergy of the fuel (kW)
$\overline{LHV}_{fuel}$	Lower heating value (kJ/kg)
φ	Chemical exergy factor
$\dot{E}x_{dest}$	Exhaust exergy rate (kW)
$\dot{E}x_{heat}$	Exergy heat loss rate (kW)
ε_{tm}	Thermo-mechanical exergy (kW)
ε_{chem}	Chemical exergy (kW)
ηt	Energy (thermal) efficiency
ψ	Exergy efficiency
S_{EG}	Entropy generation (kW/K)
P	Cost ($)
R_{thrm}	Thermoeconomic parameter (kW/$)
R_{exg}	Exergoeconomic parameter (kW/$)

Subscripts

o	Dead state (or environmental state)
in	Incoming
out	Outgoing
cw	Cooling water
gen,t	Total cost generation
ci	Capital cost
om	Operation and maintenance cost
oc	Other cost